Proceedings of the Combustion Institute, Volume 28, 2000/pp. 1471–1478

INITIATION IN H_2/O_2: RATE CONSTANTS FOR $H_2 + O_2 \rightarrow H + HO_2$ AT HIGH TEMPERATURE

J. V. MICHAEL, J. W. SUTHERLAND,* L. B. HARDING AND A. F. WAGNER

Chemistry Division
Argonne National Laboratory
Argonne, IL 60439, USA

The reaction between H_2 and O_2 has been studied in a reflected shock tube apparatus between temperatures of 1662–2097 K and pressures of 400–570 torr with Kr as the diluent gas. O atom atomic resonance absorption spectrometry (ARAS) was used to observe absolute $[O]_t$ under conditions of low $[H_2]_0$ so that most secondary reactions were negligible. Hence, the observed $[O]_t$ was the direct result of the rate controlling reaction between H_2 and O_2. Three different reactions were considered, but experimental and *ab initio* theoretical results both indicated that the process, $H_2 + O_2 \rightarrow H + HO_2$, is the most probable reaction. After rapid HO_2 dissociation, O atoms are then instantaneously produced by $H + O_2 \rightarrow O + OH$. Using the *ab initio* result, conventional transition state theoretical calculations (CTST) with tunneling corrections give the expression $k_1^{th} = 1.228 \times 10^{-18}\, T^{2.4328} \exp(-26{,}926\ K/T)$ cm^3 molecule^{-1} s^{-1}, applicable between 400 and 2300 K. This theoretical result agrees with the present experimental determinations and those at lower temperature, derived from earlier work on the reverse reaction.

Introduction

The branching chain oxidation of H_2 with O_2 is one of the most studied reactions in combustion. It was recognized very early that branching could only occur after some initiation process produces radical chain centers [1]. Over the years, five initiation reactions have been considered:

$$H_2 + O_2 \rightarrow H + HO_2 \quad (1)$$

$$H_2 + O_2 \rightarrow OH + OH \quad (2)$$

$$H_2 + O_2 \rightarrow O + H_2O \quad (3)$$

$$H_2 + M \rightarrow H + H + M \quad (4)$$

and

$$O_2 + M \rightarrow O + O + M \quad (5)$$

Reactions 1 and 2 have been the preferred initiation processes since reaction 3 requires multiple bond rearrangement and both diatomic dissociation reactions; 4 and 5 require substantially higher energy [2]. Reaction 2 was almost always the choice in shock tube induction delay experiments [3–6] until about 1985, with the value from Ripley and Gardiner [3], $k_2 = 4.16 \times 10^{-12} \exp(-19{,}605\ K/T)$ cm^3 molecule^{-1} s^{-1}, being typical. However, later flow tube studies at room temperature [7,8] on the reverse of reaction 1, $H + HO_2 \rightarrow H_2 + O_2$, gave a rate constant of $k_{-1} = 6.7 \times 10^{-12}$ cm^3 molecule^{-1} s^{-1} with at least an error of ±50%, essentially corroborating earlier values [9,10]. Using Janaf calculated equilibrium constants [11], Warnatz [12] then estimated rate constants for reaction 1 and suggested its importance as an initiation process. With derived 773 K results from Baldwin et al. [13] (i.e., $k_{-1} = 4.65 \times 10^{-11}$ cm^3 molecule^{-1} s^{-1}), Tsang and Hampson [14] further refined the estimate, albeit with a large uncertainty, suggesting $k_1 = 2.4 \times 10^{-10} \exp(-28{,}500\ K/T)$ cm^3 molecule^{-1} s^{-1} for 300–800 K.

From the above discussion, it is clear that currently used values for initiation with reactions 1, 2, or 3 are based on a relatively small experimental database. In the present work, we studied the $H_2 + O_2$ reaction with atomic resonance absorption spectrometry (ARAS) under low $[H_2]$ conditions using the reflected shock tube technique. Absolute rates of O atom formation are measured during the initial stages of reaction under conditions where the rate of initiation is rate controlling and nearly chemically isolated. Previous ARAS studies [6,15,16] did not use a sufficiently high $[O_2]/[H_2]$ ratio to allow kinetic isolation of the initiation process. The difficulty in assessing initiation with ignitable quantities of H_2 and O_2 is well illustrated in the work of Pamidimukkala and Skinner [6], who finally concluded that thermal dissociation of impurities probably initiated the branching chain oxidation in their work. By contrast, in the present work $[H_2]$ is so small and impurity levels are so low that any observed atom formation

*Present address: Guest Scientist, Department of Applied Science, Brookhaven National Laboratory, Upton, NY 11973

must derive from a direct bimolecular reaction between H_2 and O_2.

Experimental

The present experiments were performed with previously described equipment [17], and, therefore, only a brief description of the system, along with those features unique to the current experimental procedures, will be presented here.

The apparatus consists of a 7 m (4 in. o.d.) 304 stainless steel tube separated from the He driver chamber by a 0.004 in. unscored 1100-H18 aluminum diaphragm. The tube was routinely pumped between experiments to less than 10^{-8} torr (760 torr $= 1.01325 \times 10^5$ Pa) by an Edwards Vacuum Products model CR100P packaged pumping system. The velocity of the shock wave was measured with eight equally spaced pressure transducers (PCB Piezotronics, model 113A21) mounted along the downstream part of the test section of the shock tube and recorded with a 4094C Nicolet digital oscilloscope. Temperature and density in the reflected shock wave regime were calculated from this velocity. This procedure, which includes corrections for boundary layer perturbations, has been fully described elsewhere [17,18]. The digital oscilloscope was triggered by pulses derived from the last velocity gauge signal. The photometer system was radially located 6 cm from the end plate. All optics were made from MgF_2. The resonance lamp beam intensity was measured by an EMR G14 solar blind photomultiplier tube and recorded with the oscilloscope.

The technique used for the detection of the transient O atoms is atomic resonance absorption spectroscopy (ARAS). The level of light intensity in the source is so low that photoinitiation is not possible in the present experiments. In earlier work [19], an O atom curve of growth was determined using $X_{O_2} = 1 \times 10^{-3}$ in 1.8 torr of purified grade He at 50 W microwave power to give an effective lamp temperature of 490 K [20]. This curve of growth was slightly modified with the inclusion of additional data obtained in a later study [21]. The present experiments were carried out in exactly the same way as in this earlier study [21] except that H_2 was used as the reactant instead of CH_3. Following procedures discussed earlier [21], 28 kinetics experiments were carried out between 1662 and 2097 K.

Gases

High purity He (99.995%), used as the driver gas, was from Air Products and Chemicals. Scientific grade Kr (99.999%), the diluent gas in reactant mixtures, was from Spectra Gases. In Kr, the ~10 ppm impurities (N_2, 2 ppm; O_2, 0.5 ppm; Ar, 2 ppm; CO_2, 0.5 ppm; H_2, 0.5 ppm; CH_4, 0.5 ppm; H_2O, 0.5 ppm; Xe, 5 ppm; CF_4, 0.5 ppm) are all either inert or in sufficiently low concentration so as to not perturb O atom profiles. Ultra high purity grade He (99.999% from AGA Gases) was used for the resonance lamp. High purity O_2 (99.995%) for the atomic filter was from AGA Gases. Scientific grade O_2 (99.999%) and H_2 (99.9999%) for reaction mixtures were obtained from MG Industries and were used without additional purification. Test gas mixtures were accurately prepared from pressure measurements using a Baratron capacitance manometer and were stored in an all-glass vacuum line.

Results

With the relatively high levels of O_2 used in the present experiments, there is an observable absorption of the resonance light at 130 nm by molecular oxygen. Since this absorption is uniform over the O_2 bandwidth and $[O_2]$ does not significantly change during an experiment, any observed decrease in the transmitted light intensity without reactant H_2 reflects an increase in total density (due to vibrational relaxation of O_2) and/or O atom formation from $O_2 + M \rightarrow 2O + M$ at high temperature. Hence, we carried out a limited set of O_2 dissociation experiments with the same $[O_2]$ that was used in the kinetics experiments. Under conditions where O atom formation was negligible, density relaxation (generally $<250\ \mu s$ at $T > 1600$ K) was easily determined. The apparent absorbance due to the vibrational relaxation of O_2 was a small correction and was not strongly dependent on temperature. This correction was then point-by-point subtracted from the higher temperature runs where O atoms were definitely formed from dissociation as reflected in a substantial strong increase in absorption. The corrected absorbance was then converted to $[O]_t$ with the previously determined curve of growth [21]. Using the expression $k_d = R_O/2\ [O_2][M]$, where R_O is the rate of formation of O atoms (i.e., the slope from the experimental $[O]_t$ against t plots), values for k_d were determined. For $T > 2200$ K the results were within $\pm 40\%$ of those accurately determined previously by Jerig, Thielen, and Roth [22]. Hence, we have adopted their value in the kinetics model for the H_2/O_2 experiments. In the kinetics experiments, we similarly corrected for O_2 density relaxation by point-by-point subtraction. In general, the contribution of this correction was ~20%; that is, 80% of the signal was due to chemical reaction with reactant H_2. After conversion to $[O]_t$ using the curve of growth [21], O atom concentration profiles were determined, two of which are shown in Fig. 1. These experimental profiles were then compared to those generated by numerical integration of the reaction mechanism listed in Table 1.

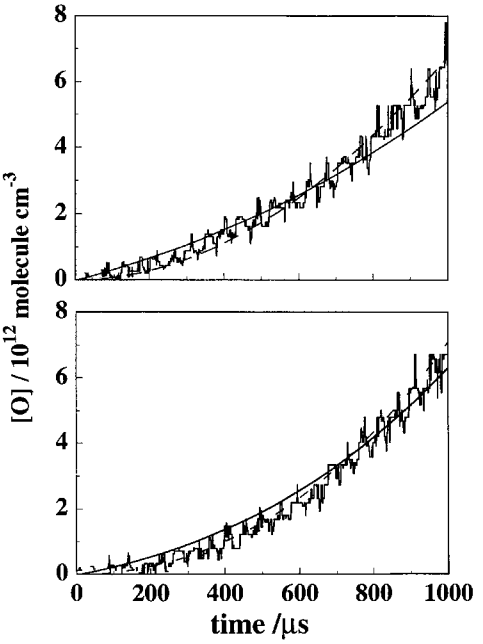

FIG. 1. Comparison of measured and simulated O atom profiles for initiation by reaction 1 (solid line) or reaction 2 (dashed line). Top panel: $P_1 = 10.94$ torr, $M_s = 2.915$, $\rho_5 = 2.549 \times 10^{18}$, $T_5 = 1981$ K, $[H_2] = 6.357 \times 10^{13}$, and $[O_2] = 1.561 \times 10^{17}$, all in molecules cm^{-3}, $k_1 = 1.6 \times 10^{-16}$ cm^3 $molecule^{-1}$ s^{-1} or $k_2 = 7.3 \times 10^{-16}$ cm^3 $molecule^{-1}$ s^{-1}. Bottom panel: $P_1 = 10.94$ torr, $M_s = 2.775$, $\rho_5 = 2.442 \times 10^{18}$, $T_5 = 1810$ K, $[H_2] = 1.227 \times 10^{14}$, and $[O_2] = 1.508 \times 10^{17}$, all in molecules cm^{-3}, $k_1 = 8.0 \times 10^{-17}$ cm^3 $molecule^{-1}$ s^{-1} or $k_2 = 2.25 \times 10^{-16}$ cm^3 $molecule^{-1}$ s^{-1}.

Discussion

Experiment

$[O]_t$ profiles (0 to 1 ms) for 28 experiments were generally simulated over the concentration range, 0 to $\sim 1 \times 10^{13}$ atoms cm^{-3}, using the mechanism of Table 1. For all conditions, the only important reactions in the table are reactions 1, 2, or 3, possibly followed by reactions 6 through 9. In the initial stages of reaction, all radical–radical processes are negligibly slow as are the reactions, H and/or O + H_2O, both of which have high activation energies. H_2 dissociation, reaction 4, is also too slow for the small $[H_2]$ employed. However, O_2 dissociation [22] can significantly contribute to O atom formation at $T > 2100$ K, and, therefore, no experiments above this temperature were included in the database. Under all experimental conditions, reactions 6 and 7 are effectively instantaneous, leaving only reactions 8 and 9 contributing to the time dependence of $[O]_t$. Hence, fitting is dependent only on the values of the rate constants for reactions 1, 2, or 3 and by reactions 8 and 9, both of which are well known over the present T range [25].

Even though most of the reactions are relatively unimportant, the entire set of reactions in Table 1 was used to simulate $[O]_t$. Fig. 1 shows two such profiles. The solid or dashed lines are simulations under the separate assumptions that reactions 1, 2, or 3 initiate the reaction. The yield of O atoms per H atom destroyed using 1 is initially 2 since both reactions 6 and 7 are instantaneous. Hence, simulations using reaction 3, where only one O atom is formed, are identical to reaction 1 except that the rate constant for reaction 3 has to be two times that for initiation by reaction 1. In all cases, the values resulted from iterative fits, and doubling or halving the rate constants for the processes results in values of $[O]_t$ at 1 ms that are about twice or one-half of those from the best fits. Given the substantial experimental error in absolute [O] (i.e., $\sim \pm 15\%$)[21], the fits give rate constant values with an estimated accuracy of $\sim \pm 20\%$. Inspection of Fig. 1 shows that reactions 1, 2, or 3 (or a combination) could account for the results, and, therefore, we determined rate constant values for the entire set of experiments using each of the three reactions as the initiation process. Starting with reaction 2, if this reaction is presumed to be the initiation process then the derived rate constants follow the Arrhenius expression $k_2 = 1.01 \times 10^{-8} \exp(-33{,}056\ K/T)$ cm^3 $molecule^{-1}$ s^{-1}, whereas, with reaction 1, the value is

$$k_1 = 1.50 \times 10^{-11} \exp(-22{,}905\ K/T)\ cm^3\ molecule^{-1}\ s^{-1} \quad (6)$$

for $1662 \leq T \leq 2097$ K. Considering reaction 3, if this were the initiation process then the only important reaction would be reaction 3 alone, and, in this case, the values for k_3 would be ~ 2 times equation 6. Since the data are obtained over such a limited T range, deciding between reactions 1, 2, and 3 is impossible from just these results alone. A choice might be possible by examining A factors and activation energies from the three analyses. If reactions 2 or 3 were operative, then one would expect low A factors (i.e., $\sim 10^{-12}$ cm^3 $molecule^{-1}$ s^{-1}) for four-center or tight transition states, respectively [27], but much higher values, $A_2 \sim 1 \times 10^{-8}$ or $A_3 \sim 3 \times 10^{-11}$ cm^3 $molecule^{-1}$ s^{-1}, are required to explain the data. Moreover, it is also worth noting that reaction 2, for parallel geometry, violates Woodward–Hoffman rules. Hence, from the experimental evidence, we consider reaction 1, summarized in equation 6, as the most likely initiation process. The rate constants derived on this basis are listed in Table 2. Due to space limitations, the conditions of these experiments are not given but can be requested from J. V.

TABLE 1
Mechanism Used for Fitting [O] Profiles from $H_2 + O_2$[a]

1.	$H_2 + O_2 \rightarrow H + HO_2$	k_1 = fitted
2.	$H_2 + O_2 \rightarrow OH + OH$	$k_2 = 0$[b]
3.	$H_2 + O_2 \rightarrow O + H_2O$	$k_3 = 0$[b]
4.	$H_2 + Kr \rightarrow H + H + Kr$	$k_4 = 8.86 \times 10^{-10} \exp(-48321\ K/T)$[c]
5.	$O_2 + Kr \rightarrow O + O + Kr$	$k_5 = 2.66 \times 10^{-6}\ T^{-1} \exp(-59380\ K/T)$[d]
6.	$H + O_2 \rightarrow OH + O$	$k_6 = 1.62 \times 10^{-10} \exp(-7474\ K/T)$[e]
7.	$HO_2 + Kr \rightarrow H + O_2 + Kr$	$k_7 = 2.0 \times 10^{-5}\ T^{-1.18} \exp(-24363\ K/T)$[f]
8.	$OH + H_2 \rightarrow H_2O + H$	$k_8 = 3.56 \times 10^{-16}\ T^{1.52} \exp(-1736\ K/T)$[e]
9.	$O + H_2 \rightarrow OH + H$	$k_9 = 8.44 \times 10^{-20}\ T^{2.67} \exp(-3167\ K/T)$[e]
10.	$OH + OH \rightarrow O + H_2O$	$k_{10} = 7.19 \times 10^{-21}\ T^{2.7} \exp(1251\ K/T)$[e]
11.	$OH + O \rightarrow O_2 + H$	$k_{11} = 5.42 \times 10^{-13}\ T^{0.375} \exp(1112\ K/T)$[e]
12.	$H + H_2O \rightarrow OH + H_2$	$k_{12} = 1.56 \times 10^{-15}\ T^{1.52} \exp(-9249\ K/T)$[e]
13.	$O + H_2O \rightarrow OH + OH$	$k_{13} = 7.48 \times 10^{-20}\ T^{2.7} \exp(-7323\ K/T)$[e]
14.	$H + HO_2 \rightarrow H_2 + O_2$	$k_{14} = k_1/K_{eq}$[g]
15.	$H + OH \rightarrow H_2 + O$	$k_{15} = 3.78 \times 10^{-20}\ T^{2.67} \exp(-2226\ K/T)$[e]

[a]All rate constants are in cm^3 $molecule^{-1}$ s^{-1}.
[b]Values taken to be 0; see text.
[c]Refs. [23,24].
[d]Ref. [22].
[e]Ref. [25].
[f]Refs. [14,26].
[g]Calculated from equation 7.

Michael. Experimental corroboration of the exclusive importance of reaction 1 is not possible by observing H atoms because reaction 6 is effectively instantaneous with the levels of O_2 necessary to measure the title reaction. Experimental corroboration by observing OH is impractical since OH is a product in both schemes, also, the low sensitivity for detection in comparison to ARAS precludes designing a chemical isolation experiment, that is, reactions 10 and 11 then become important.

Equation 6 can be compared to earlier evaluations. This equation gives values that agree well within a factor of 2 with those of Tsang and Hampson [14] over the experimental T range, 1600–2100 K. The values from Koike [16] range from 3 to 20 times higher, and those from Skinner et al. [28] are substantially lower than those calculated from equation 6. From our experimental results, we therefore conclude that reaction 1 is the most probable process responsible for initiation in the H_2/O_2 system. In the theoretical discussion to follow, this conclusion will be further assessed in terms of *ab initio* determinations of potential energy surfaces for all processes. Subsequently, conventional transition state theoretical (CTST) estimates of the thermal rate behavior will be presented and compared with experiment.

Theory

The electronic structure calculations focus on locating transition states for reactions 1 to 3. Hence, preliminary searches were made by employing low levels of theory which allow large volumes of configuration space to be explored, and then, when a given transition state is located, the structure is reoptimized at higher and more accurate levels of theory. All calculations employ the Dunning correlation–consistent basis sets [29–31]. The preliminary searches were made using the polarized valence double zeta basis set (cc-pvdz) and the critical stationary points were re-examined using the polarized quadruple zeta (cc-pvqz) basis set. Searches were carried out with both coupled cluster, CCSD(T) [32], and complete active space, self-consistent field, CASSCF [33,34], calculations. The CCSD(T) method is the most accurate, single-reference, *ab initio* method currently available. The CASSCF calculations were done to check on the possibility of transition state structures located in regions not well described by single-reference wave functions. In the CASSCF calculations reported here, all valence electrons were taken as active except the oxygen 2s electrons. The active space thus consists of 8 orbitals and 10 electrons (1512 configuration state functions). All calculations were carried out using the MOLPRO package of codes [35].

A transition state for reaction 1 was readily located. At the highest level of theory used (i.e., CCSD(T)/cc-pvqz), the structure is as follows: R_{OO} = 1.30Å, R_{OHa} = 1.05Å, R_{OHb} = 2.24Å, HaOO∠ = 107.1°, and HbOO∠ = 107.7°. As expected for an endothermic reaction, the transition state is very

TABLE 2
High Temperature Rate Data for $H_2 + O_2$

T/K	$k_1/(cm^3\ molecule^{-1}\ s^{-1})$
2097	3.0 (−16)
1927	9.0 (−17)
1897	9.0 (−17)
1907	2.0 (−16)
1848	1.0 (−16)
2063	2.5 (−16)
1981	1.6 (−16)
1826	1.0 (−16)
1960	1.0 (−16)
1819	3.2 (−17)
1851	3.0 (−17)
1891	1.1 (−16)
1810	8.0 (−17)
1679	5.0 (−17)
1948	1.5 (−16)
1974	1.1 (−16)
1963	1.3 (−16)
2002	1.4 (−16)
1881	8.0 (−17)
1844	9.0 (−17)
1698	1.5 (−17)
1838	4.2 (−17)
1819	2.6 (−17)
1785	2.0 (−17)
1662	1.6 (−17)
1704	1.5 (−17)
1950	9.0 (−17)
1822	4.0 (−17)

"late" with an OH bond extension of only 0.08Å, relative to HO_2 and an HH bond extension of 0.45Å, relative to H_2. The calculated, in-plane, harmonic frequencies are 1717, 1374, 1169, 321, and 1825i cm^{-1}. These can be compared to calculated frequencies for $H_2 + O_2$ of 4403 and 1600 cm^{-1} and, for HO_2, of 3672, 1441, and 1142 cm^{-1}. For the out-of-plane bending mode of the transition state, it was not possible to do calculations at the CCSD(T)/cc-pvqz level. For this mode we use the result of a CCSD(T)/cc-pvdz calculation, namely, 681 cm^{-1}.

The calculated barrier, without zero point corrections, is 57.8 kcal mol^{-1}. For comparison, calculations with cc-pvdz and cc-pvtz basis sets give barriers of 60.2 and 58.3 kcal mol^{-1}. Most of the decrease in barrier height with increasing basis set size correlates with a decreasing endothermicity, that is, the small reverse barrier is less sensitive to the level of theory. The calculated reverse barriers are 2.9, 2.6, and 2.7 kcal mol^{-1} using cc-pvdz, cc-pvtz, and cc-pvqz basis sets, respectively.

Regarding the cc-pvqz zero point corrected endothermicity for reaction 1, 55.4 kcal mol^{-1} is obtained, and this value is in excellent agreement with recent measurements by Litorja and Ruscic [36], 55.7 ± 0.8 kcal mol^{-1}. This new endothermicity [36] is 2.8 kcal mol^{-1} higher than used by Janaf [11], and therefore the Janaf estimated equilibrium constants are ~1.64 to 100 times larger than implied by Litorja and Ruscic, from 2500 down to 300 K. With the harmonic oscillator approximation, K_{eq} for reaction 1 can be calculated using these experimental results [36], giving to within ±3%

$$K_{eq} = 0.2021\ T^{0.3455} \exp(-27656\ K/T) \quad (7)$$

between 300 and 2500 K. K_{eq} can also be calculated from the present theory, and there is only a few percent difference between theory and experiment, corroborating the accuracy of the present *ab initio* results.

Extensive searches (i.e., $\sim 10^5$ points) of both planar and non-planar (including perpendicular) geometries were also made for the transition states of reactions 2 and 3. The searches were carried out at both the CCSD(T)/cc-pvdz and CASSCF/cc-pvdz levels. No transition state for either reaction could be found. While the existence of a transition state connecting any two minima on a multidimensional potential surface is guaranteed, the existence of a *direct* transition state is not. Previous calculations [37] have shown the existence of indirect pathways for both reactions 2 and 3, that is, $H_2 + O_2 \rightarrow H + HO_2 \rightarrow H_2O + O \rightarrow 2OH$. In symmetry-restricted searches where only geometries possessing a plane (or more) of symmetry are considered, high lying saddle points can be located for both reactions 2 and 3. However, when the symmetry restriction is relaxed it is found that these are not true saddle points because they have two or more imaginary normal mode frequencies. The mode corresponding to one of the imaginary frequencies can be identified with reaction coordinates for reactions 2 or 3. The mode corresponding to one of the other imaginary frequency leads down to the transition state for 1. This suggests a potential energy landscape in which the $H_2 + O_2$ minimum is surrounded by a multidimensional ridge, the low point of which is the transition state for reaction 1. Thus, the picture that emerges from these calculations is that the lowest energy pathways for reactions 2 and 3 are stepwise processes in which the first step is reaction 1.

The final part of this theoretical treatment is a CTST calculation of the rate of reaction 1 using the unadjusted *ab initio* barrier height, structures, and frequencies given above. We note that the RMS deviation between the calculated and observed frequencies for the reactants and products is less than 30 cm^{-1}, justifying the use of unscaled frequencies. These calculations were carried out using the VARIFLEX program [38], within a rigid-rotor, harmonic oscillator approximation. Tunneling estimates were made using both Wigner and Eckart methods. The Wigner and Eckart tunneling estimates are found to

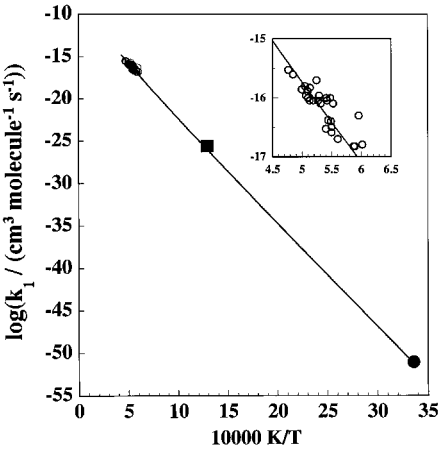

FIG. 2. Arrhenius plot of the data for k_1. Open circles, data from Table 1. The line is the *ab initio* theoretical calculation summarized by the three-parameter expression, equation 8. Closed square, data of Ref. [13], and closed circle, data of Refs. [7–10], both transformed using equation 7. Inset: open circles, data from Table 2. The line is the theoretical calculation summarized by equation 8.

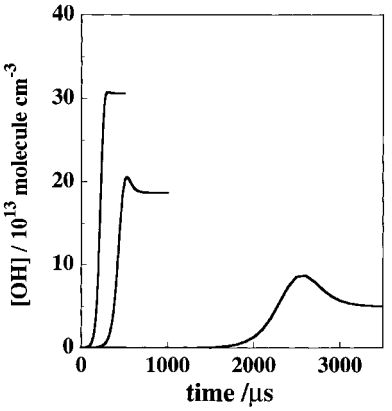

FIG. 3. A simulation of OH profiles at three temperatures (from left to right, 1927, 1700, and 1300 K, respectively), using the mechanism of Table 1 with the theoretical value for k_1 as given by equation 8. The total density is 1.326×10^{18} with $[H_2] = 6.524 \times 10^{16}$ and $[O_2] = 6.522 \times 10^{15}$ (all in molecules cm^{-3}) for all three simulations. The simulation at 1927 K reproduces the experimental data reported as figure 4 from Ref. [48].

be very similar, increasing the rate at 300 K by a factor of 3, while contributing only 10% at 1000 K and less than 1% at 2000 K. Both the experimental (points) and the theoretical (line) results of the present study are shown in Fig. 2 as an Arrhenius plot. The theoretical line in the figure can be expressed to within ±2% by the three-parameter equation:

$$k_1^{th} = 1.228 \times 10^{-18}\, T^{2.4328} \exp(-26926\ K/T)\ cm^3\ molecule^{-1}\ s^{-1} \quad (8)$$

over the temperature range, 400–2300 K. Experimental data from previous work [7–10,13] on the reverse reaction (−1) have been transformed from k_{-1} to k_1 using the revised K_{eq}, equation 7. Note that the values transformed refer only to the back reaction as reported [7–10,13] and do not include the predominate process, $H + HO_2 \rightarrow 2OH$ (estimated to be 92 ± 4% at room temperature [7–10]). The completely *ab initio* result summarized by equation 8 is remarkably consistent with experiment over the entire T range.

Conclusion

On both experimental and theoretical grounds, we therefore conclude that reactions 2 and 3 can be ignored and that only reaction 1 initiates chain branching in the H_2/O_2 system. The theoretical prediction of the rate behavior derived from first principles agrees with experiment over an extended T range. We therefore recommend that the theoretical result, equation 8, should be exclusively used in modeling the branching chain oxidation of H_2. The remaining question to be answered is then whether this k_1 value can supply sufficient O atom rates for the branching chain oxidation to occur. As is well known, ignition-delay-type experiments have traditionally monitored OH radical production [23,39–48]. Using the mechanism of Table 1 along with equation 8, we simulated typical oxidation experiments at three temperatures. These simulations are shown in Fig. 3, and, in all cases, chain branching was clearly demonstrated. The experimental conditions for the 1927 K simulation are from this laboratory [48], and it is worth noting that the present simulation reproduces the experimental data shown in figure 4 from this earlier study. The other two simulations were carried out at the same total density, $[H_2]$, and $[O_2]$ with the only change being in the temperature. Even at 1300 K with an incomplete mechanism, rates of H and HO_2 formation calculated from equation 8 are large enough to initiate branching chain oxidation, although requiring a considerably longer induction time. Hence, we conclude that reaction 1 is sufficient to initiate H_2 oxidation by O_2.

Acknowledgments

This work was supported by the U.S. Department of Energy, Office of Basic Energy Sciences, Division of Chemical Sciences, under contract no. W-31-109-Eng-38.

REFERENCES

1. Semenov, N., *Acta Physicochim. U. R. S. S.*, 20:291–302 (1945).

2. Bradley, J. N., *Shock Waves in Chemistry and Physics,* Wiley, New York, 1962, p. 307.
3. Ripley, D. L., and Gardiner Jr., W. C., *J. Chem. Phys.* 44:2285–2296 (1966).
4. Belles, F. E., and Brabbs, T. A., *Proc. Combust. Inst.* 13:165–174 (1971).
5. Jachimowski, C. J., and Houghton, W. M., *Combust. Flame* 17:25–30 (1971).
6. Pamidimukkala, K. M., and Skinner, G. B., *Thirteenth International Symposium on Shock Waves and Shock Tubes,* State University of New York, Albany, 1981, pp. 585–592.
7. Sridharan, U. C., Qui, L. X., and Kaufman, F., *J. Phys. Chem.* 86:4569–4574 (1982).
8. Keyser, L. F., *J. Phys. Chem.* 90:2994–3003 (1986).
9. Hack, W., Preuss, A. W., Wagner, H. Gg., and Hoyermann, K., *Ber. Bunsen-Ges. Phys. Chem.* 83:212–217 (1979).
10. Thrush, B. A., and Wilkinson, J. P. T., *Chem. Phys. Lett.* 84:17–19 (1981).
11. Chase Jr., M. W., Davies, C. A., Downey Jr., J. R., Frurip, D. J., McDonald, R. A., and Syverud, A. N., *J. Phys. Chem. Ref. Data* 14:Supplement no. 1 (1985).
12. Warnatz, J., in *Combustion Chemistry,* (W. C. Gardiner Jr., ed.), Springer, Heidelberg, Germany, 1984, p. 197.
13. Baldwin, R. R., and Walker, R. W., *Proc. Combust. Inst.* 17:525–532 (1979); Baldwin, R. R., Fuller, M. E., Hillman, J. S., Jackson, D., and Walker, R. W., *J. Chem. Soc. Faraday Trans. 1* 70:635–641 (1974).
14. Tsang, W., and Hampson, R. F., *J. Phys. Chem. Ref. Data* 15:1087–1279 (1986).
15. Frank, P., and Just, Th., *Ber. Bunsen-Ges. Phys. Chem.* 89:181–187 (1985).
16. Koike, T., *Bull. Chem. Soc. Jpn.* 62:2480–2483 (1989).
17. Michael, J. V., *J. Chem. Phys.* 90:189–198 (1989).
18. Michael, J. V., and Sutherland, J. W., *Int. J. Chem. Kinet.* 18:409–436 (1986).
19. Michael, J. V., and Lim, K. P., *J. Chem. Phys.* 97:3228–3234 (1992).
20. Maki, R. G., Michael, J. V., and Sutherland, J. W., *J. Phys. Chem.* 89:4815–4821 (1985).
21. Michael, J. V., Kumaran, S. S., and Su, M.-C. *J. Phys. Chem.* 103:5942–5948 (1999).
22. Jerig, L., Thielen, K., and Roth, P., *AIAA J.* 29:1136–1139 (1991).
23. Du, H., and Hessler, J. P., *J. Chem. Phys.* 96:1077–1092 (1992).
24. Michael, J. V., Kumaran, S. S., Su, M.-C., and Lim, K. P., *Chem. Phys. Lett.* 319:99–106 (2000).
25. Michael, J. V., *Prog. Energy Combust. Sci.* 18:327–347 (1992).
26. Mallard, W. G., Westley, F., Herron, J. T., Hampson, R. F., *NIST Chemical Kinetics Database, Ver. 6.0,* NIST Standard Reference Data, Gaithersburg, MD (1994).
27. Benson, S. W., *Thermochemical Kinetics, 2nd ed.,* Wiley, New York, 1976.
28. Skinner, G. B., Lifshitz, A., Scheller, K., and Burcat, A., *J. Chem. Phys.* 56:3853–3861 (1972).
29. Dunning Jr., T. H., *J. Chem. Phys.* 90:1007–1023 (1989).
30. Kendall, R. A., Dunning Jr., T. H., and Harrison, R. J., *J. Chem. Phys.* 96:6796–6806 (1992).
31. Woon, D. E., and Dunning Jr., T. H., *J. Chem. Phys.* 98:1358–1371 (1993).
32. Hampel, C., Peterson, K., and Werner, H.-J., *Chem. Phys. Lett.* 190:1–12 (1992), and references therein.
33. Werner, H.-J., and Knowles, P. J., *J. Chem. Phys.* 82:5053–5063 (1985).
34. Knowles, P. J., and Werner, H.-J., *Chem. Phys. Lett.* 115:259–267 (1985).
35. Werner, H.-J., and Knowles, P. J., with contributions from Almlof, J., Amos, R. D., Berning, A., Cooper, D. L., Deegan, M. J. O., Dobbyn, A. J., Eckert, F., Elbert, S. T., Hampel, C., Lindh, R., Lloyd, A. W., Meyer, W., Nicklass, A., Peterson, K., Pitzer, R., Stone, A. J., Taylor, P. R., Mura, M. E., Pulay, P., Schutz, M., Stoll, H., and Thorsteinsson, T., *MOLPRO package of ab initio programs.* http://www.tc.bham.ac.uk/molpro/.
36. Litorja, M., and Ruscic, B., *J. Electron Spectrosc.* 97:131–146 (1998).
37. Harding, L. B., in *Advances in Molecular Electronic Structure Theory,* (T. H. Dunning Jr., ed.), JAI Press, Greenwich, CT, 1990, p. 45.
38. Klippenstein, S. J., Wagner, A. F., Robertson, S. H., Dunbar, R. C., and Wardlaw, D. M., *VARIFLEX, Version 1.0,* http://chemistry.anl.gov/variflex; VARIFLEX is a freeware program package for calculating gas phase reaction rates.
39. Bird, P. F., and Schott, G. L., *J. Quant. Spectrosc. Radiat. Transfer* 5:783–811 (1965); Schott, G. L., and Getzinger, R. W., in *Physical Chemistry of Fast Reactions,* (P. B. Levitt, ed.), Plenum, London, 1973, p. 81, and references cited therein.
40. Bradley, J. N., Capey, W. D., Fair, R. W., and Pritchard, D. K., *Int. J. Chem. Kinet.* 8:549–561 (1976).
41. Jachimowski, C. J., and Houghton, W. M., *Combust. Flame* 15:125–132 (1970).
42. Gardiner Jr., W. C., Mallard, W. G., and Owen, J. H., *J. Chem. Phys.* 60:2290–2295 (1974).
43. (a) Ernst, J., Wagner, H. Gg., and Zellner, R., *Ber. Bunsen-Ges. Phys. Chem.* 81:1270–1275 (1977); (b) Ernst, J., Wagner, H. Gg., and Zellner, R., *Ber. Bunsen-Ges. Phys. Chem.* 82:409–414 (1978); (c) Niemitz, K. J., Wagner, H. Gg., and Zellner, R., *Z. Phys. Chemie* NF124:155–170 (1981).
44. (a) Hanson, R. K., Salimian, S., Kychankoff, G., and Booman, R. A., *Appl. Opt.* 21:641–643 (1983); (b) Rea Jr., E. C., Chang, A. Y., and Hanson, R. K., *J. Quant. Spectrosc. Radiat. Transfer* 37:117–127 (1987); (c) Masten, D. A., Hanson, R. K., and Bowman, C. T., *J. Phys. Chem.* 94:7119–7128 (1990).

45. Yuan, T., Wang, C., Yu, C.-L., Frenklach, M., and Rabinowitz, M. J., *J. Phys. Chem.* 95:1258–1265 (1991).
46. (a) Fujii, N., and Shin, K. S., *Chem. Phys. Lett.* 151:461–465 (1988); (b) Yang, H., Gardiner Jr., W. C., Shin, K. S., and Fujii, N., *Chem. Phys. Lett.* 231:449–453 (1994).
47. (a) Ryu, S.-O., Hwang, S. M., and Rabinowitz, M. J., *Chem. Phys. Lett.* 242:279–284 (1995); (b) Ryu, S.-O., Hwang, S. M., and Rabinowitz, M. J., *J. Phys. Chem.* 99:13984–13991 (1995).
48. Su., M.-C., Kumaran, S. S., Lim, K. P., and Michael, J. V., *Rev. Sci. Instrum.* 66:4649–4654 (1995).

COMMENTS

P. R. Westmoreland, University of Massachusetts, USA. What value was used for the heat of formation of HO_2?

Author's Reply. The value used is from M. Litorja and B. Ruscis [1]; they report $\Delta H^{\circ}_{f,0k} = (4.0 \pm 0.8)$ kcal mole^{-1} ($\Delta H_{f,298K} = (3.3 \pm 0.8)$ kcal mole^{-1}).

REFERENCE

1. Litorja, M., and Ruscis, B., *J. Electron Spectrosc.* 97:131–146 (1998).